Lithology and Mineral Resources, Vol. 35, No. 5, 2000, pp. 434–444. Translated from Litologiya i Poleznye Iskopaemye, No. 5, 2000, pp. 487–499.

Glauconite from Lower Cretaceous Marine Terrigenous Rocks of England: A Concept of Biochemogenic Origin

A. R. Geptner and T. A. Ivanovskaya

Geological Institute (GIN), Russian Academy of Sciences, Pyzhevskii per. 7, Moscow, 109017 Russia

Received January 31, 2000

Abstract—Detailed mineralogical characteristics of various forms of glauconite occurrence in Lower Cretaceous marine terrigenous rocks of the White Island (Binnel Bay, southern England) are discussed. It has been shown that glauconite was formed *in situ* due to the transformation of fine-dispersed and sandy–silty terrigenous materials. The influence of bacterial activity on glauconite formation is supported by the study of dissolution zones on quartz and feldspar grains, which revealed biomorphic structures akin to fossilized bacteria.

INTRODUCTION

The active role of bacteria in the formation of some mineral materials is known for a long time and was especially emphasized in a great number of recent publications. Factors, which determine the activity of microorganisms and their impact on the formation and destruction of minerals in various environments, were comprehensively discussed by Ehrlich (1996). Carbonates, Fe-, Mn-, and Si-minerals, as well as phosphates are mostly chosen as subjects for the investigation of bacterial contribution to mineral formation (Castanier *et al.*, 1989; Gorshkov *et al.*, 1992; Gerasimenko *et al.*, 1996; Konhauser and Ferris, 1996). Data on the important role of microorganisms in the hydrothermal formation of layer silicates were reported by Köhler *et al.* (1994) and Tazaki (1997). The participation of bacteria in the glauconite formation in modern and ancient sediments was exemplified by Geptner *et al.* (1994) and Geptner and Ivanovskaya (1998).

Results of the investigation of Lower Cretaceous glauconite-bearing marine rocks reported in this paper furnish evidence for the active microbial impact on the formation of various forms of glauconite occurrence and related glauconization of terrigenous silicate material (quartz and feldspar).

MATERIALS AND METHODS

The glauconite sandstone sample was taken in 1989 from the coast of White Island (Binnel Bay, southern England). According to the personal communication of P.P. Timofeev who kindly placed the sample at our disposal, the sandstone is related to shallow-water coastal sediments at the Aptian–Albian boundary.

Glauconite grains were singled out from the rock by the following procedure. The weakly cemented rock was crushed by a rubber pestle up to a friable state, sieved, washed, and dried at room temperature. Grain size fractions were separated into samples with density ranging from 2.4 to 2.9 g/cm^3 with a step of 0.05 g/cm^3. Then the glauconite was separated from terrigenous components with a SIM-1 electromagnetic separator.

Glauconite grains were studied under an optical microscope and scanning electron microscope. Additionally, they were examined by the chemical microanalysis, X-ray method, and infrared spectroscopy. The research was accompanied by a petrographical study of the rock. Some components, including the clay fractions (<0.6 and <1 μm) were investigated by the X-ray method. Chemical compositions of different-density glauconite grains, glauconite and clay terrigenous cement, as well as biomorphic material were determined by scanning electron microscope equipped with a Link-860 microprobe.

The X-ray analysis was performed by E.V. Pokrovskaya; the chemical microanalysis, by K.A. Stepanova; and the SEM study of glauconite and terrigenous grains, by the authors in collaboration with N.V. Gor'kova (GIN). The microprobe study was carried out in collaboration with L.T. Protasevich at the Paleontological Institute, RAS.

CHARACTERISTICS OF THE SAMPLE

The sample consists of greenish gray, weakly cemented, medium to fine-grained sandstone and siltstone (Fig. 1). The discontinuous thin horizontal bedding (lamina thickness does not exceed 1 mm) is emphasized by a variable amount of glauconite grains (from 1–2 to 80%) in intercalating bands. A mud-eater trail, up to 2 cm long and 0.6 cm wide, filled with terrigenous material and sparse glauconite grains was noticed. The outer rim of the trail is rather well-cemented.

The terrigenous material is mainly composed of quartz and insignificant amount of feldspars (5–10%) and muscovite (≤1%). Green, greenish brown, and brown flakes (biotite?) and less abundant coal frag-

0024-4902/00/3505-0434$25.00 © 2000 MAIK "Nauka/Interperiodica"

ments of fine silt size are sporadically dispersed throughout the rock.

Glauconite occurs as shape-variable grains and fine-dispersed matrix, which fills fissures and replaces terrigenous fragments to a variable extent. As can be seen in thin sections, glauconite grains are closely intergrown, and isolated grains are less abundant.

In monomineral bands, glauconite grains are incorporated into the glauconite matrix and not always may be clearly distinguished against the matrix background, because the grain boundaries are not distinctly delineated; moreover, the microstructure (and color) of glauconite grains and matrix are similar. One can observe clearly visible, expanded, sand- and silt-size mica flakes that are partly replaced by glauconite and incorporated into the glauconite matrix. They are green in the transmitted light and reveal pleochroism and high interference color inherent in biotite. Numerous muscovite flakes often remain unaltered.

In the course of petrographic study, the special attention was paid to relationships between glauconite, relics of clayey terrigenous material, and sandy–silty fragments. Sketches and photomicrographs presented in Fig. 2 demonstrate the relationships of glauconite grains, matrix, and terrigenous material. Most terrigenous grains are angular and distinctly corroded. This is clearly seen where irregular quartz or feldspar grains intrude the glauconite matrix to a variable extent. Glauconite also penetrates the feldspar along fractures and the quartz–feldspar aggregate along grain boundaries. In the case of intensive corrosion by glauconite, the formerly intact grains are destroyed and represented by angular fragments separated by glauconite. However, the primary contour of terrigenous grains can be readily restored by the character of twinning and extinction.

The terrigenous clay material is only seen within limited areas of thin section between glauconite and terrigenous grains. In the transmitted light, the clay material represents a dark or light brown fine-dispersed substance locally containing a great amount of fine-dispersed, opaque organic (?) particles. In the reflected light, the clay material sometimes bears a violet tint and silky luster. It should be noted that the clay material is distinguished by a nonuniform (bleached or pale green) color in different areas of thin section. Such areas are characterized by an intense aggregate polarization. Quartz grains are corroded at contacts with the bleached and pale green clay material.

Within the mud-eater trail, the terrigenous grains are covered and cemented by a thin film of iron hydroxide with microglobular texture observed under the scanning electron microscope. In addition to sparse grains of green glauconite, a fine-dispersed, brown with a violet shade (in reflected light) material is detected in the intergranular space of the inner zone of the mud-eater trail. Based on the X-ray analysis, the clay minerals are represented by dioctahedral mica, smectite, and kaolinite (Fig. 3a). The dioctahedral mica is referred to as Fe-illite (lattice parameter b is ~9.00 Å).

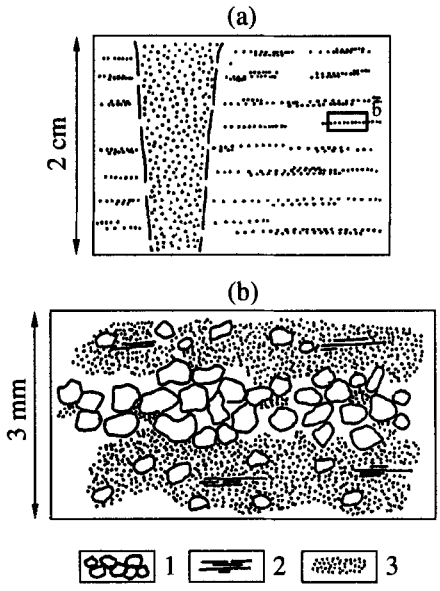

Fig. 1. (a) Bedding and mud-eater trail in the sample and (inset b) distribution of terrigenous material and glauconite in the thin section. The legend for inset b: (1) terrigenous material consisting of quartz and less abundant feldspar fragments; (2) muscovite; (3) glauconite mass composed of globules and cement.

As was shown by the microprobe, the brown fine-dispersed material with a violet shade is inhomogeneous in composition. In particular, the domains enriched in Cl (possibly of chlorides K and Na) have been only detected within the fine-dispersed terrigenous material (Fig. 4).

Clay separates of <0.6 and <1.0 μm are mainly represented by dioctahedral hydromica (expanding layers 10–20%) having a tendency to the ordering of mica and smectite layers (short-range order factor, S > 1). Kaolinite is noticed as an admixture (Fig. 3b). Judging from the b value of 9.06 Å, the hydromica is represented by the Al–Fe variety (glauconite).

GENERAL MORPHOLOGICAL FEATURES OF GLAUCONITE

The **shape** of glauconite, as was mentioned above, is diverse. Both glauconite grains and matrix were studied in detail. Most abundant grain types with a sequentially complicated morphology are as follows: (1) rounded, oval, and kidney-shaped globules with an even surface, (2) grains with a knobby (close to globular) surface, and (3) palmate and brain-shaped varieties with prominent knobs on the surface. The globule morphology can be complicated by relationships with surrounding terrigenous grains, the penetration of fractures to a variable depth, or the polyglobular (aggregate) structure. Polyglobular aggregates are

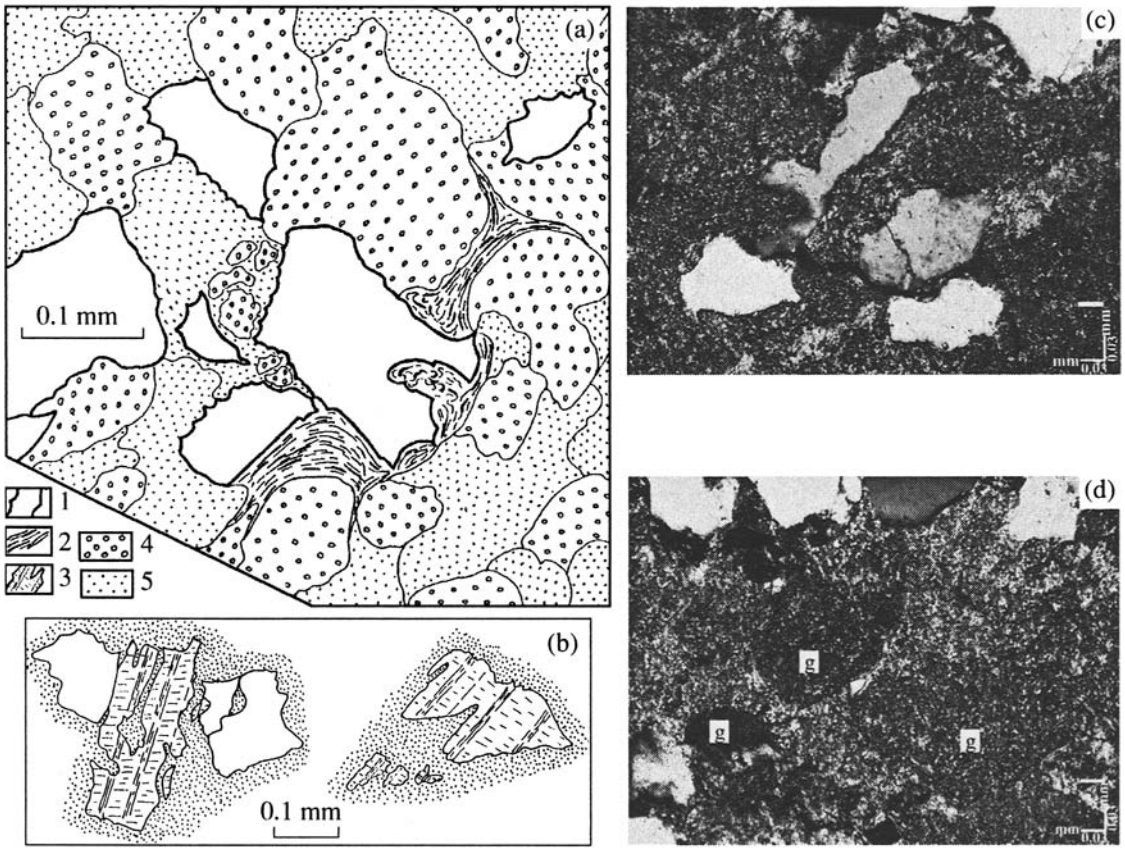

Fig. 2. (a, b) Sketches and photomicrographs (c, d) of thin sections demonstrating the relationship of terrigenous sandy–silty and fine-dispersed materials with authigenic glauconite. Sketches (a, b): (1) quartz, (2) feldspar, (3) light brown fine-dispersed terrigenous material; (4) dark green globular glauconite; (5) light green globules and glauconite matrix. Photomicrographs: (c) corroded quartz and quartzite grains in the light green glauconite matrix; (d) dark green globular glauconite (g) in light green glauconite matrix. Bar in (c) and (d) is 0.03 mm.

represented by cemented globules of various sizes, e.g., two kidney-shaped grains cemented by a light-colored mass or several small globules held together by a matrix. The amount of glauconite matrix in such aggregates varies in a wide range.

The glauconite matrix in the intergranular space is characterized by irregular shapes, dull or slightly silky luster, and lower hardness (in comparison with glauconite globules with a glossy surface, which is especially typical of heavy fractions).

In some glauconite grains, one side has rounded outlines and glossy surface, whereas another side resembles the glauconite matrix. In thin sections, such grains are separated from the matrix by a distinct contour on one side and a gradual transition on another side.

The **size** of single grains and their aggregates varies from 0.6 to 1.0 mm. We can identify the following proportions of grain-size fractions: 0.6–0.315 mm (1%), 0.315–0.20 mm (5%), 0.20–0.16 mm (10%), 0.16–0.10 mm (42%), and 0.10–0.05 mm (42%). Additionally, each fraction contains glauconite matrix fragments resulted from the destruction and separation of the sample. A few small globules can be incorporated into such fragments. It should be noted that the high content (42%) of fine fraction (<0.1 mm) is caused by mechanical destruction of various glauconite grains and aggregates, which have a very low hardness.

The **density** of glauconite in separate grain-size fractions (0.6–0.2, 0.2–0.16, 0.16–0.10 mm) varies from 2.4 to 2.8 g/cm^3. The lightest (2.40–2.45 g/cm^3) and the heaviest (2.65–2.80 g/cm^3) grains are minor (1–3%). Grains with a density of 2.45–2.60 g/cm^3 dominate (87–90%) in the fractions listed above.

The **color** of prevalent glauconite grains is yellowish green. The color intensity varies from light to dark green with transition from light to heavy fractions. The matrix content also decreases from light to heavy fractions. In the same density fraction, in comparison with grains, the matrix is distinguished by a lighter color. The matrix and grains are occasionally similar in color. The least amount of matrix fragments and the greatest amount of globular (oval, rounded, and kidney- and brain-shaped) grains are contained in density fractions of 2.65–2.70 and 2.70–2.80 g/cm^3.

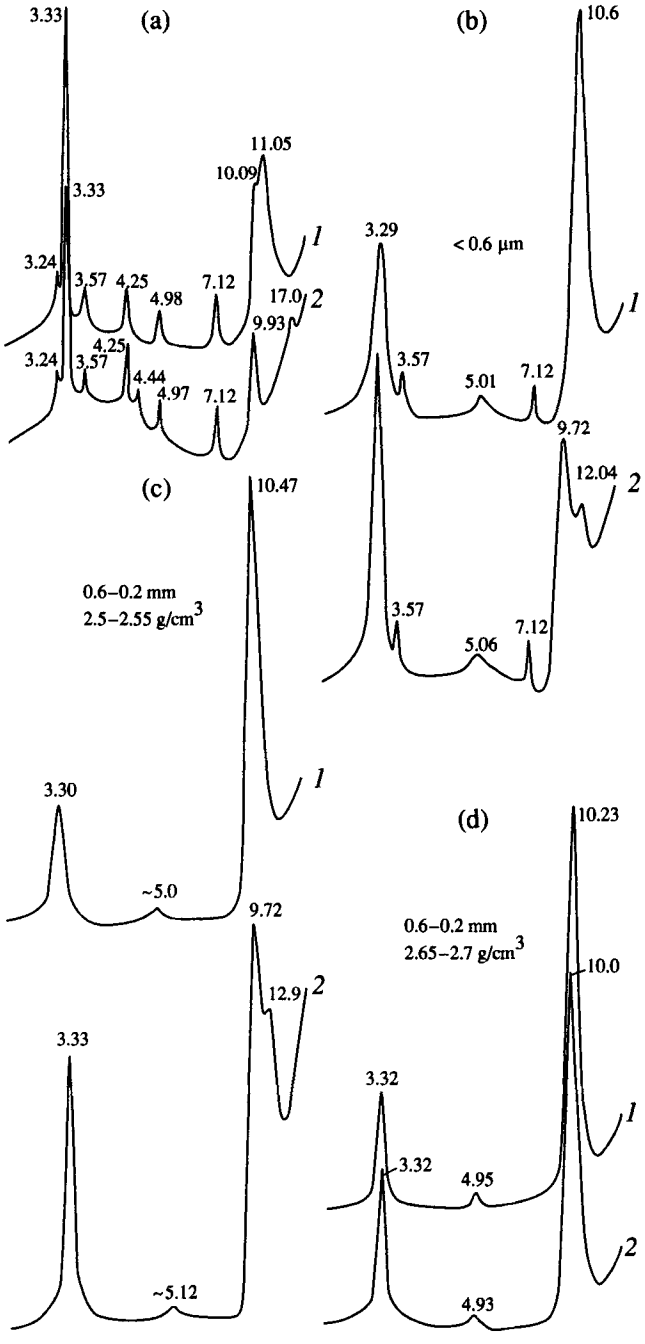

Fig. 3. X-ray patterns of oriented specimens. (a) Fragments of fine-dispersed terrigenous material (>0.6 mm); (b) <0.6 μm fraction; (c) light fraction (2.50–2.55 g/cm^3) grains; (d) heavy fraction (2.65–2.75 g/cm^3) grains. Samples: (*1*) air-dried; (2) saturated with ethylene glycol.

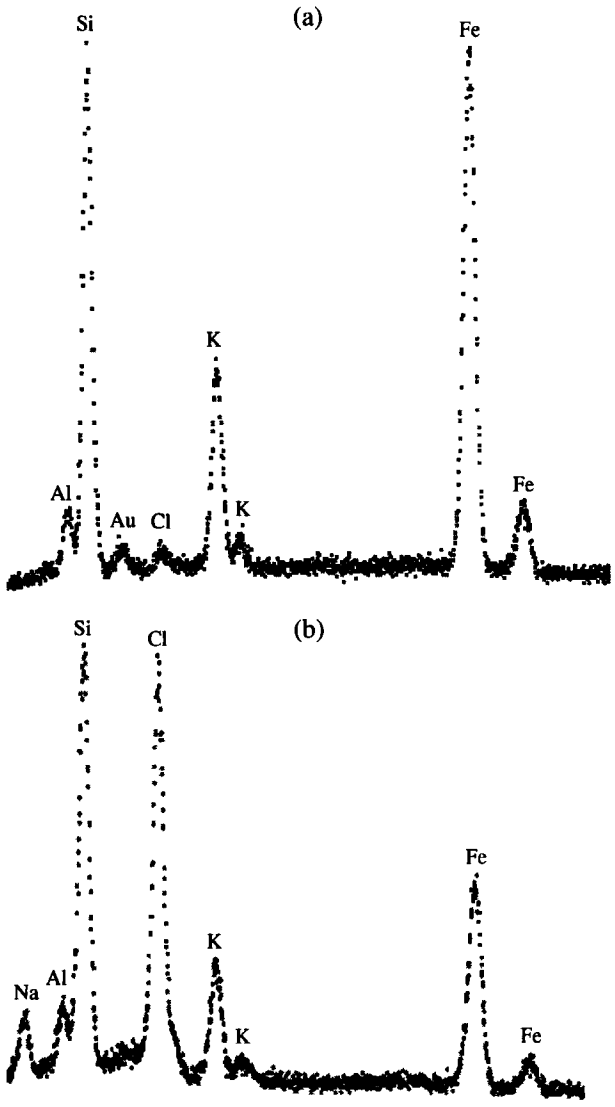

Fig. 4. Microprobe data. (a) Fine-dispersed terrigenous material; (b) microinclusions in terrigenous material.

X-RAY DATA

Based on X-ray patterns of oriented specimens, grains from light fractions (2.40–2.50, 2.50–2.55, and 2.55–2.60 g/cm^3) are represented by hydromicas (expanding layers 10–20%). The X-ray diffraction patterns of specimens saturated with organic fluids reveal the reflection with d ~11.3–12.9 Å in combination with the 001 reflection with d ~9.7–9.8 Å, indicating an ordered alternation of mica and smectite layers in the hydromica (S > 1). Let us recall that precisely these density fractions are predominant in the sample. The heavier fractions (2.60–2.65, 2.65–2.70, and 2.70–2.80 g/cm^3) are represented by micaceous minerals proper (expanding layers 5–10%). This fact is illustrated by X-ray patterns of two density fractions (Figs. 3c, 3d).

It is interesting that the micaceous minerals are slightly different in the content of expanding layers even in one density fraction. For example, dark globules in the 2.65–2.70 g/cm^3 fraction, which are distinguished by a higher magnetic susceptibility, are characterized by a lower content of expanding layers, relative to more light-colored varieties and cement fragments.

The reflection with d = 1.513 Å (b = 9.078 Å) registered on the powder X-ray pattern of grains (0.6–0.2 mm,

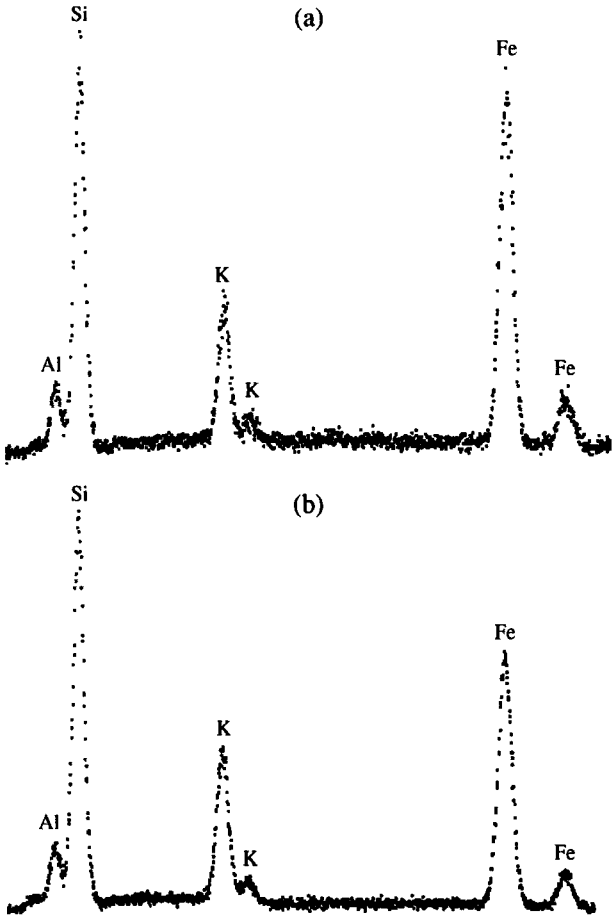

Fig. 5. Microprobe data. (a) Dark green globules; (b) light green glauconite cement.

2.45–2.65 g/cm^3) in the $d(060)$ region matches the dioctahedral micaceous mineral of glauconite composition. The presence of defects in glauconite (1Md polytype, $n60°$) is evaluated by the K coefficient (Drits *et al.*, 1993). The value of this coefficient for the glauconite under study is 0.22, suggesting an abundance of defects.

CRYSTAL CHEMISTRY AND SPECTROSCOPY

The comparative chemical analysis with the application of a Link-860 microprobe revealed an almost identical distribution of Si, Fe, Al, and K in micaceous minerals from various density fractions (Fig. 5). This implies that the density variation and respective color change are not related to Fe and K contents in minerals.

Based on the complete chemical microanalysis, the composition of grains, 0.6–0.2 mm in size and 2.45–2.65 g/cm^3 in density, is as follows (wt %): SiO_2 (50.71), Al_2O_3 (9.48), Fe_2O_3 (19.79), FeO (1.31), MgO (1.91), CaO (0.53), Na_2O (0.45), K_2O (6.11), H_2O^+ (5.91), H_2O^- (3.00), total (99.20). Formula units were calculated on the basis of constant anion framework $(O_{10}(OH)_2)^{-22}$ for a half of unit cell:

$$K_{0.58}Na_{0.06}Ca_{0.04}[Fe^{3+}_{1.09}Al_{0.56}Fe^{2+}_{0.08}Mg_{0.21}]_{1.94}[Si_{3.74}Al_{0.26}]_4.$$

As can be seen from the formula, the Fe^{3+} cation prevails over Al cation in octahedral sites of 2 : 1 layers of the micaceous mineral. The $Fe^{3+}/(Fe^{3+} + Al)$ ratio (n) is 0.66. According to the classification proposed by Tsipurskii and Ivanovskaya (1988), the micaceous mineral is referred to as glauconite ($n \geq 0.5$). The total cation charge of 2 : 1 layers is equal to 0.72 v.u., and the K content amounts to 0.58 f.u. The octahedral cation charge (0.47 v.u) is higher than that of tetrahedral charge (0.26 v.u.).

The IR-pattern of the sample reveals one strong band with the maximum at ~3530 cm^{-1} ($Fe^{3+}Fe^{2+}$) and a very weak band with the maximum at ~3600 cm^{-1} (MgAl) in the region of OH-group oscillations. Such a proportion of band intensities fits the Fe-rich (glauconitic) composition of the dioctahedral micaceous mineral.

NANOSTRUCTURE STUDY

The scanning electron microscope was applied to study the following subjects: (1) rock fragments, (2) particular quartz, feldspar, and glauconite grains, and (3) glauconite globules from various density fractions (2.45–2.50, 2.60–2.65, 2.65–2.70, and 2.70–2.80 g/cm^3). Both globule sections and surfaces were investigated. A special attention was paid to relationships between terrigenous grains and glauconite matrix.

The internal nanostructure of globules is rather diverse. Four nanostructural types are recognized. In the first (cellular or honeycomb) type, flakes on cell walls surround the holes of various shapes and sizes (Fig. 6a). In the second type, the flakes are gathered in "rosettes" (Fig. 6b). The third type is characterized by a compact internal structure with a chaotic (or less frequently oriented) distribution of flakes that are occasionally slightly curved and grouped into peculiar fans (Fig. 6c). In addition, the globules include compact homogeneous clusters with poorly discernible flakes and random voids (fourth type of nanostructure). The rectangular contours of such voids cast no doubt that they inherited the shape of older terrigenous fragments of fine silty dimension (Fig. 6d). All the above nanostructural types can occasionally be seen within one globule. Such patterns are typical of both light and heavy fractions.

The nanostructure of grain surface is also diverse. In one case, rosettes or fans of smoothed flakes are observed on the surface (Figs. 7a, 7b). A thin rim of closely packed flakes oriented nearly perpendicular to the surface can be observed on the section (Fig. 7c). In another case, the surface is represented by a shell of several tangentially oriented flakes, which envelops the internal nanostructure of globule (Figs. 7d–7f).

The globule surface is often crosscut by fissures of different depths and configurations. The grains crosscut

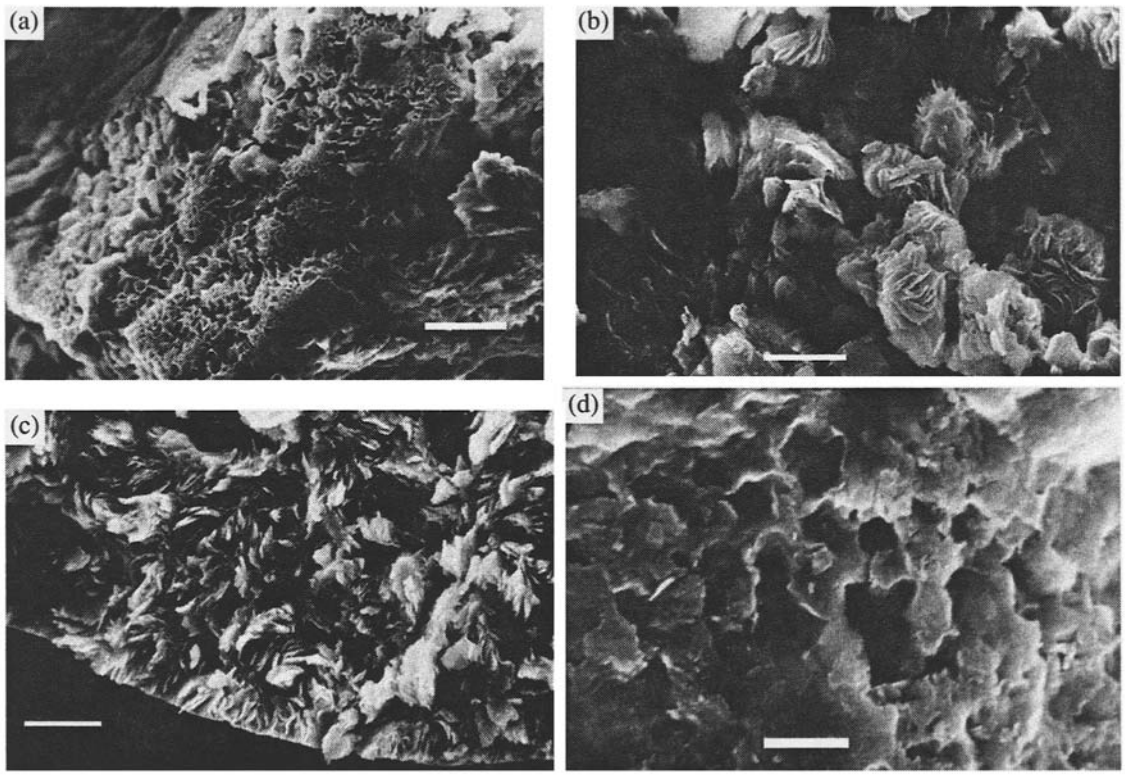

Fig. 6. Nanostructures of globular glauconite. (a) Honeycomb; (b) rosettes; (c) fans; (d) homogeneous structures with holes left behind the dissolved terrigenous fragments. Bar is 10 μm in (a, b, d) and 4 μm in (c).

by deep fissures have a brain-shaped surface. Fissures may be open or filled with glauconite matrix (Figs. 8a–8d). Open fissures are subdivided into two types. Fissures of the first type have walls with a retained internal structure of the globule. Fissures of the second type have walls and margins covered by clay flakes (Fig. 8c), which turn into the outer shell mentioned above.

Signs of dissolution of terrigenous material of sandy and silty dimensions are particularly numerous in the glauconite matrix holding the glauconite globules (Figs. 9a–9d). The dissolution of terrigenous material and contemporaneous glauconite formation is clearly demonstrated by the development style of glauconite flakes in some hollows on the surface of terrigenous fragments. The flakes can form aggregates enveloping irregularities in partly dissolved terrigenous grains and penetrate the fragments along fractures (Fig. 9b). An irregular dissemination of small pyrite crystals can also be observed on the corroded surfaces of quartz and feldspar grains.

Numerous objects, which resemble the fossilized bacteria in shape and size, were detected on the surface of terrigenous fragments with clear indications of dissolution (Figs. 9c, 9d, 10a–10d). They are represented by slightly curved bars with rounded endings. Occasionally, they form small rings or spheres with a hole in the middle (Figs. 10a–10d). The size of such formations is constant (3 μm in length and 1 μm in diameter). Small glauconite flakes, which are commensurable with biomorphic structures, are also observed. The microprobe analysis has shown that the biomorphic structures contain Al, Fe, and K, which were not detected on the grain surface beyond the dissolution zone (Fig. 11). Thus, the biomorphic structures are fossilized and contain the same components that were detected in the dark and light green glauconite grains from heavy and light fractions, respectively. Similar results were obtained by the analysis of corroded surface of quartz grain with numerous clots of fossilized microbial forms. The analysis of individual bacterial forms is hampered by their small dimensions.

GENESIS OF GLAUCONITE

Despite the long-term research of glauconite, the problem of its genesis remains a matter of debate. New mineralogical data presented above, including the nanostructural features and relationships with terrigenous material, provide additional insights into the possible mechanism of glauconite formation.

The dioctahedral 2 : 1 layer silicate—glauconite is abundant in the terrigenous rocks under study. The parameter *b* of glauconite is 9.08 Å. The mineral is represented by both mica and hydromica varieties. The latter, as was mentioned above, are characterized by specific diffraction patterns ($S > 1$). The Fe^{3+} cation prevail

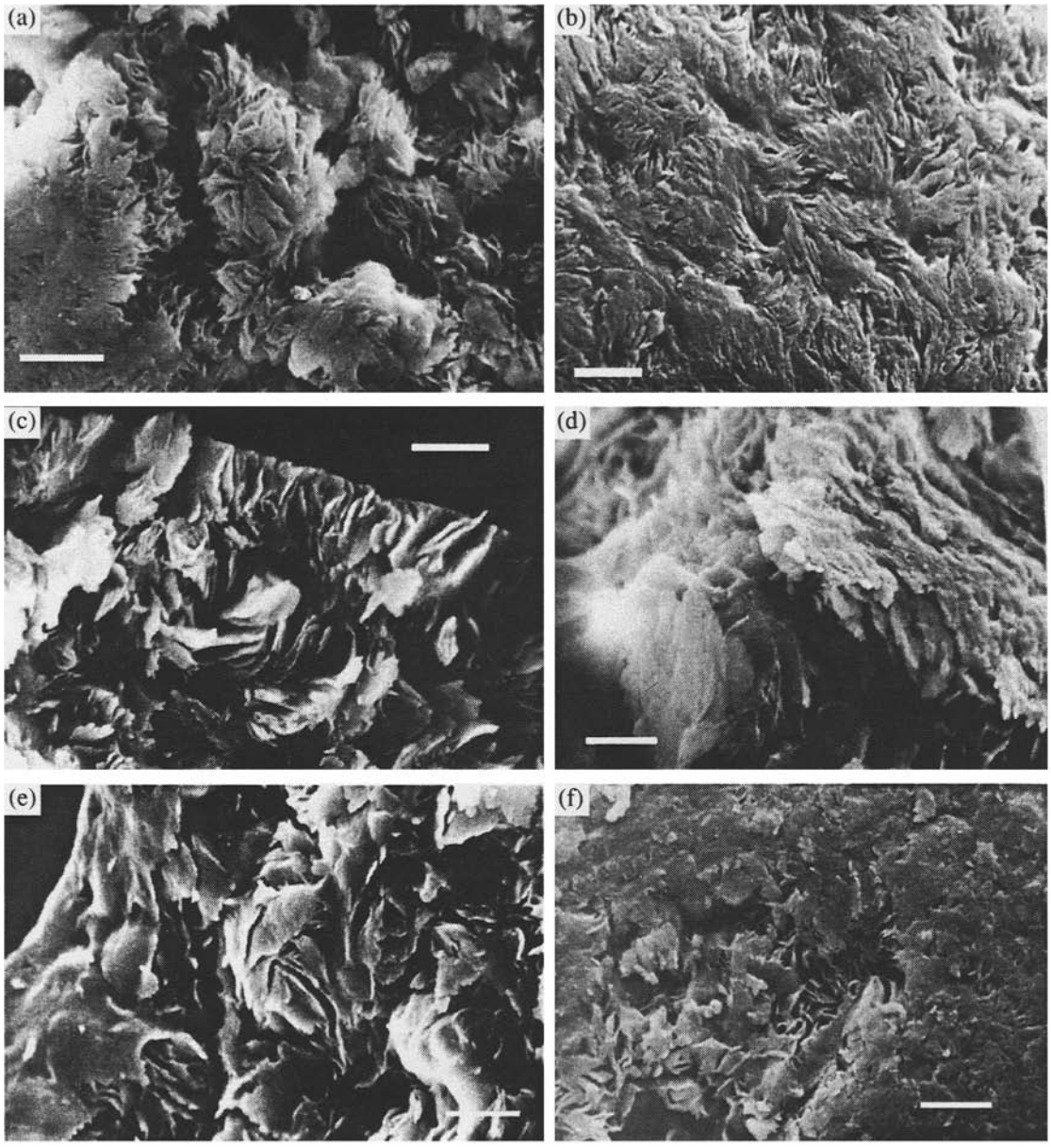

Fig. 7. Nanostructures on the surface of globular glauconite. (a) Rosettes with flattened flakes on the globule surface; (b) fan-shaped nanostructure of the globule surface; (c) globule section: fan-shaped nanostructure of the inner part of globule gives way to a narrow rim toward the surface; the rim consists of closely packed flakes oriented nearly perpendicular to the globule surface; (d–f) shell composed of flakes oriented tangentially to the globule surface; the internal honeycomb structure is seen in (f). Bar is 4 μm in (a, f) and 2 μm in (b–e).

over Al in octahedral sites 2 : 1 (Fe^{3+}_{VI} is 1.09 f.u. and Al_{VI} is 0.56 f.u.). The octahedral charge is higher than the tetrahedral one. The K content in mineral is not high (0.58 f.u.). Such a low K content, which is unusual for micaceous minerals, is rather typical of the glauconite-series minerals in younger and older rocks. Therefore, the glauconite is referred to as a low-charged mica (Tsipurskii and Ivanovskaya, 1988).

The glauconite forms globules, fine-dispersed matrix, fills fissures, and replaces terrigenous fragments to a variable extent. Let us consider the evidence in favor of the authigenic origin of glauconite.

The glauconite is unevenly distributed in the rock. Enriched (glauconite up to 80%) and depleted (mainly terrigenous grains) bands are intercalating. However, this fact cannot be interpreted as a result of enrichment of sediment in glauconite grains during the rewashing and redeposition, because glauconite globules vary in size, density, shape, color, and relationships with the glauconite matrix. Clastic glauconite was not found in thin sections. Small grain fragments in fractions were

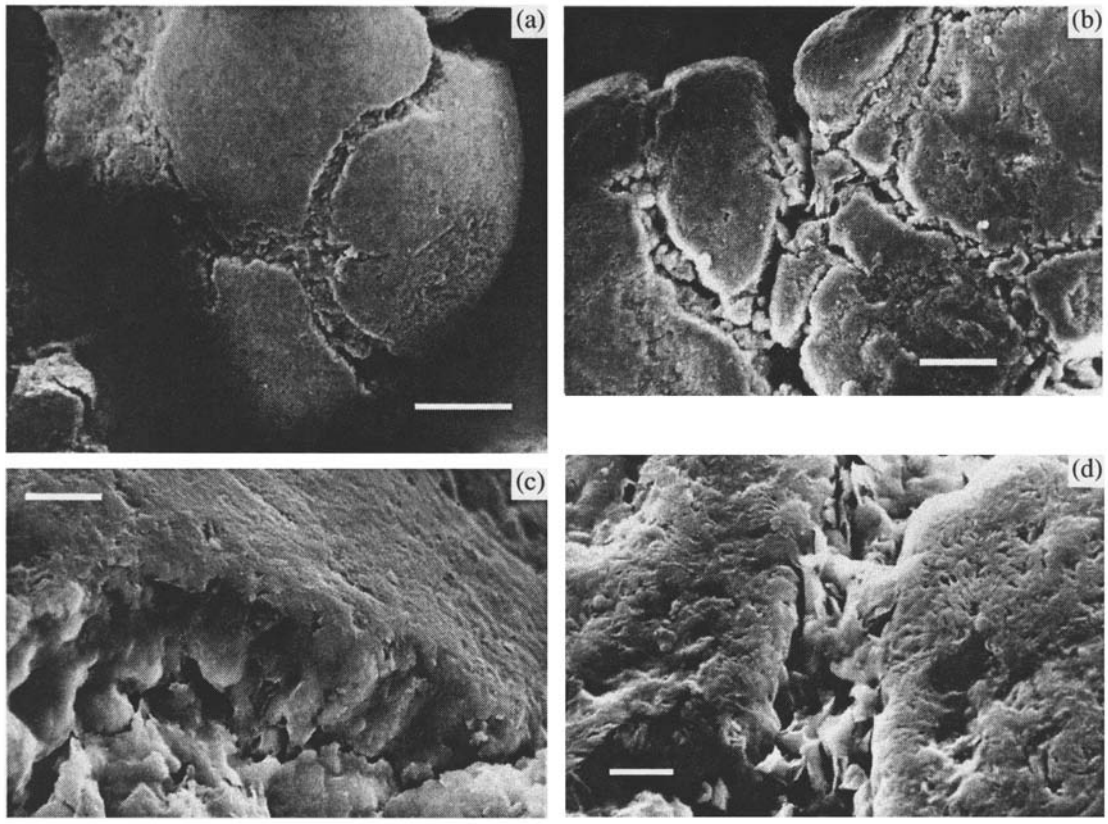

Fig. 8. Morphology and structure of fissures in dark green globules. (a) Fissure filled with glauconite; (b) open fissures partly filled with glauconite and sparse terrigenous grains; (c) globule surface and the fissure wall enveloped by glauconite; (d) fissure filled with glauconite. Bar is 40 μm in (a), 20 μm in (b), and 4 μm in (c, d).

formed as a result of mechanical destruction in the course of sample separation.

Aggregates along with fractured, palmate and brain-shaped globules with a rough knobby surface are not related to rewashing. Fissures, which locally penetrate the globules to a significant depth, are filled with glauconite flakes that cover the fissure walls or extend on the globule surface. All the above features and the grading of some globules into the glauconite matrix point to the authigenic nature of globular glauconite and the contemporaneous formation of glauconite matrix.

Severely expanded, greenish brown biotite (?) sheets, which are partly replaced by glauconite and encountered near the glauconite grains, could have hardly been rewashed. Strongly corroded (and sometimes disintegrated) quartz and feldspar fragments in glauconite matrix exclude a possibility of redeposition and substantial deformation of sediment after the formation of glauconite globules and matrix. This fact serves as evidence for the *in situ* formation of glauconite in the sediment. Some sectors of the brown clayey terrigenous material are bleached and transformed into light green patches characterized by an aggregate polarization of clay material due to the inferred gradual glauconitization. The destruction and replacement of clastic materials during glauconite formation are well known from old and recent sediments (Lisitsina and Butuzova, 1979, 1981; Geptner and Ivanovskaya, 1998). In our case, this process is indicated by numerous signs of the dissolution of quartz and feldspar grains, the glauconitization of mica sheets, and the substantial compositional difference between fine-dispersed terrigenous and authigenic materials (including glauconite). Clay minerals in the terrigenous material are represented by Fe-illite (b = 9.00 Å), smectite, and kaolinite. The enrichment in Cl and the presence of Na or K at such sites was proved by the microprobe analysis. It is inferred that chlorides could be derived from connate seawater. At the same time, Cl was not detected either in globules (b = 9.08 Å) or in glauconite matrix (b = 9.06 Å). This rules out the late supply of Cl into coastal cliff rocks of the surf zone together with seawater. Otherwise, Cl should be absorbed by glauconite as well. It is reasonable to suggest that the lack of Cl in glauconite is related to the dissolution of all terrigenous components and the removal of some chemical elements by groundwater.

The formation of glauconite in the zone of dissolution and replacement of terrigenous siliceous grains in Upper Eocene marine sediments of southern England was thoroughly discussed by Hughes and Whitehead (1987). Based on microscopic and microprobe studies,

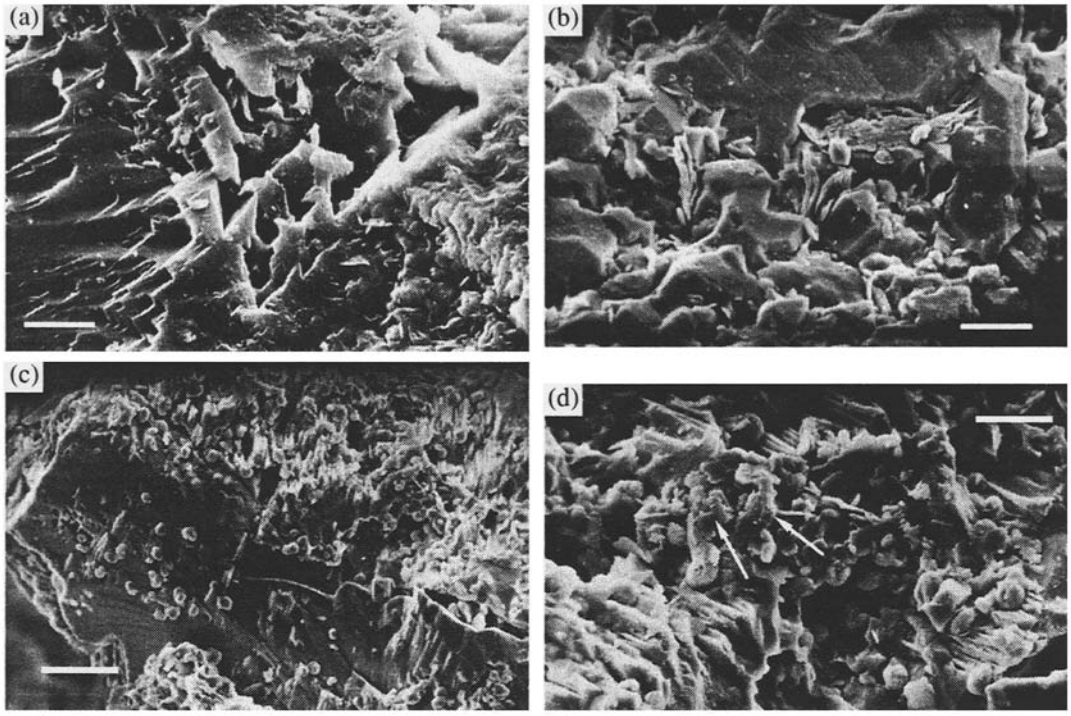

Fig. 9. Dissolution of (a, b, d) feldspar and (c) quartz grains replaced and cemented by glauconite. (a) Corroded feldspar grain; (b) corroded feldspar grain partly replaced by glauconite; (c) corroded quartz grain with small (rounded) fossilized bacteria on surface; (d) rounded fossilized bacteria on the surface of corroded feldspar grain and adjacent glauconite flakes (arrows). Bar is 4 μm.

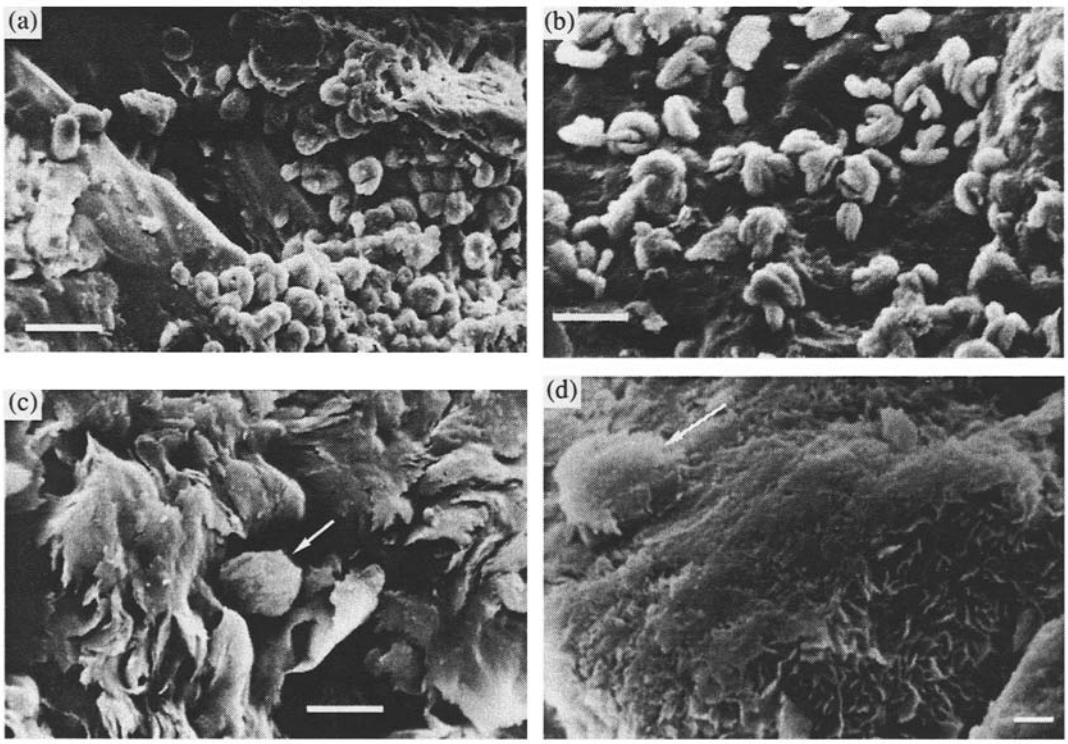

Fig. 10. Fossilized bacteria (a, b) on the surface of corroded terrigenous grains, (c) inside glauconite globule, and (d) on their surface as shown by arrows. Bar is 4 μm in (a, d) and 2 μm in (b, c).

they demonstrated that the glauconite formation zone is characterized by the sequential replacement of siliceous grains by layer silicates and the gradual formation of glauconite globules (pellets). It should be noted that microprobe data on the altered surface of siliceous fragment in the quoted work and our own results on the corroded surface of quartz grain and fossilized bacteria from the Cretaceous rock are strikingly similar (Fig. 11).

The role of bacteria in the destruction of various silicate minerals was experimentally investigated (Yakhontova *et al.*, 1983). It was established that quartz is destroyed by silicate bacteria even in the neutral water solution. The quartz with a defective structure is most intensively leached. These researchers pointed out that "...although common principles and regularities govern the abiogenic and biogenic destruction of quartz, the bacterial factor prompts a more intensive development of the process and accomplishes it even under nearly neutral conditions that are unfavorable for the abiogenic system." (Yakhontova *et al.*, 1983, p. 32).

The presence of fossilized bacteria and their accumulations in zones of terrigenous fragment dissolution suggests that microorganisms played a significant role in the dissolution of large fragments and clayey terrigenous material during the formation of glauconite. Spherical biomorphic structures, 4 to 6 μm in diameter, which were found inside one glauconite grain among the fan-shaped flake aggregate (Fig. 10c) and on the surface of another glauconite grain (Fig. 10d), furnish evidence for the participation of microorganisms in the formation of glauconite globules. In both cases, the synchronous formation of glauconite and fossilization of biomorphic structures is indicated by small flakes of clay minerals, which envelop such structures.

The intense and often complete replacement of the terrigenous material by glauconite hampers the recognition of particular stages in the continuous glauconization. The available data show that glauconite could be formed in Cretaceous marine sediments in the same way as was established for recent sediments in the Pacific Ocean (Geptner and Ivanovskaya, 1998). The globular glauconite started to form at local sites. Subsequently, the glauconitization spread over the major volume of sediments. Previously formed globules continued to grow up together with an extensive development of other varieties. At the same time, the terrigenous material was replaced and the glauconite matrix was produced at adjacent sites.

The similar alteration and replacement of terrigenous material by glauconite in Cretaceous and Upper Eocene rocks of the study region, coupled with literature and our data on other regions, where the same relationships between terrigenous material and glauconite have been observed, indicate that glauconite formation at the expense of terrigenous material is a dominating but not a unique process. The microbial activity is most important for the initiation and execution of this process.

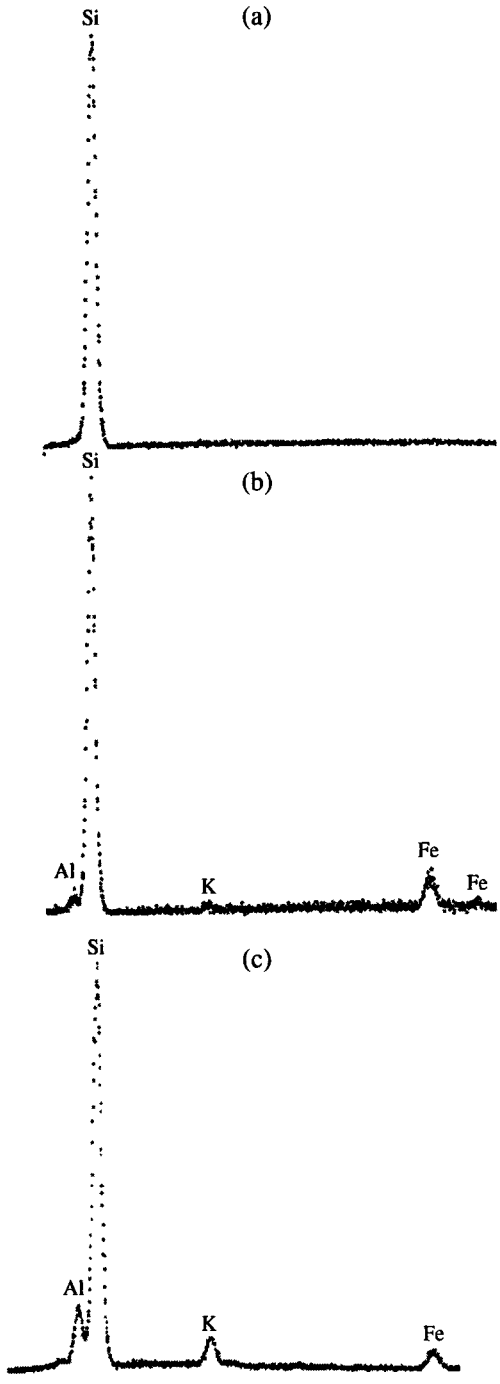

Fig. 11. Correlation of microprobe data on (a) intact, (b) corroded quartz surface with fossilized bacteria, and (c) large biomorphic structure (inferred bacterial colony) on the quartz surface.

CONCLUSIONS

Glauconite is abundant in Lower Cretaceous terrigenous rocks of southern England (White Island, Binnel Bay). The mineral occurs as rounded, oval, kidney-shaped, and brain-shaped grains and prevails in the clayey matrix of sandstones and siltstones. It corrodes the terrigenous quartz and feldspar fragments.

The crystallochemical formula of glauconite in globules is as follows:

$$K_{0.58}Na_{0.06}Ca_{0.04}[Fe^{3+}_{1.09}Al_{0.56}Fe^{2+}_{0.08}Mg_{0.21}]_{1.94}[Si_{3.74}Al_{0.26}]_4.$$

Its parameter b is 9.08 Å. The mineral is represented by both micaceous and hydromicaceous varieties. The hydromicaceous variety reveals specific diffraction patterns ($S > 1$) in both matrix and globules.

Glauconite was formed *in situ* due to the crystallization of Fe–Si gels, which were produced with an active participation of microorganisms during the alteration of terrigenous material at different rates in various portions of the sedimentary material.

The presence of fossilized microbial forms in glauconite-bearing rocks and their paragenetic relations to corroded terrigenous grains and authigenic glauconite indicate that the biochemogenic process played a leading role in the formation of glauconite globules and matrix.

ACKNOWLEDGMENTS

This work was supported by the Russian Foundation for Basic Research, project nos. 99-05-65338 and 99-05-64054.

REFERENCES

Castanier, S., Maurin, A., and Perthuisot, J.-P., Production bacterienne expérimentale de corpuscules carbonatés, sphéroidaux á structure fibro-radiaire. Réflexions sur la définition des ooides, *Bull. Soc. Géol. France*, 1989, vol. 5, no. 3, pp. 589–595.

Drits, V.A., Kameneva, M.Yu., Sakharov, B.A., Dainyak, L.G., Tsipurskii, S.I., Smolyar, B.B., Bukin, A.S., and Salyn, A.I., *Problemy opredeleniya real'noi struktury glaukonitov i rodstvennykh tonkozernistykh fillosilikatov* (Problems of Determination of the Real Structure of Glauconites and Related Fine-Grained Phyllosilicates), Novosibirsk: Nauka, 1993.

Ehrlich, H.L., *Geomicrobiology*, New York: Marcel Dekker, 1996.

Geptner, A.R. and Ivanovskaya, T.A., Biochemogenic Genesis of the Glauconite–Nontronite Series Minerals in Present-Day Sediments of the Pacific Ocean, *Litol. Polezn. Iskop.*, 1998, no. 6, pp. 563–580 [*Lithol. Miner. Resour.* (Engl. Transl.), 1998, no. 6, pp. 503–517].

Geptner, A.R., Ivanovskaya, T.A., and Ushatinskaya, G.U., Problem of the Biochemogenic Origin of Glauconite–Illite Phyllosilicates, *Litol. Polezn. Iskop.*, 1994, no. 1, pp. 79–91.

Gerasimenko, L.M., Gonchakova, I.V., Zhegallo, E.A., Zavarzin, G.A., Zaitseva, L.V., Orleanskii, V.K., Rozanov, A.Yu., Tikhomirova, N.S., and Ushatinskaya, G.T., Filamentous Cyanobacteriae: The Process of Mineralization (Phosphatization), *Litol. Polezn. Iskop.*, 1996, no. 2, pp. 208–214 [*Lithol. Miner. Resour.* (Engl. Transl.), 1996, no. 2, pp. 185–190].

Gorshkov, A.I., Drits, V.A., Dubinina, G.A., Bogdanova, O.A., and Sivtsov, A.V., Role of Bacterial Activity in the Formation of Hydrothermal Fe–Mn Rocks in the Northern Lau Basin (Southwestern Pacific Ocean), *Izv. Ross. Akad. Nauk, Ser. Geol.*, 1992, no. 9, pp. 84–93.

Hughes, A.D. and Whitehead, D., Glauconitization of Detrital Silica Substrates in the Barton Formation (upper Eocene) of the Hampshire Basin, Southern England, *Sedimentology*, 1987, vol. 34, pp. 825–835.

Köhler, B., Singer, A., and Stoffers, P., Biogenic Nontronite from Marine White Smoker Chimneys, *Clays Clay Miner.*, 1994, vol. 42, no. 6, pp. 689–701.

Konhauser, K.O. and Ferris, F.G., Diversity of Iron and Silica Precipitation by Microbial Mats in Hydrothermal Waters, Iceland: Implication for Precambrian Iron Formations, *Geology*, 1996, vol. 24, no. 4, pp. 323–326.

Lisitsina, N.A. and Butuzova, G.Yu., Authigenic Minerals in Sediments of the World Ocean, *Litol. Polezn. Iskop.*, 1979, no. 4, pp. 29–42.

Tazaki, K., Biomineralization of Layer Silicates and Hydrated Fe/Mn Oxides in Microbial Mats: An Electron Microscopical Study, *Clay Clay Miner.*, 1997, vol. 45, no. 2, pp. 203–212.

Tsipurskii, S.I. and Ivanovskaya, T.A., Crystal Chemistry of Globular Layer Silicates, *Litol. Polezn. Iskop.*, 1988, no. 1, pp. 41–49.

Yakhontova, L.K., Nesterovich, L.G., Lyubarskaya, G.A., Andreev, P.I., Pyzhov, V.Kh., and Blinova, G.K., Desintegration of Silicates with the Help of Bacteria, *Mineral. Zn.*, 1983, vol. 5, no. 2, pp. 28–38.